

CHARACTERISATION OF THE HEAT AFFECTED ZONE OF MULTILAYER WELDS

Aleksandar Sarić

voestalpine Böhler Welding Austria GmbH, Kapfenberg, Austria

Key words: *Heat affected zone, CB2, 9% chromium steel, MatCalc, multilayer welds, Gleeble, instrumented impact test*

Abstract:

This work deals with the analysis of simulated heat affected zone (HAZ) in gas metal arc welding (GMAW) welding of the 9% chromium steel CB2. The HAZ was simulated and characterised by means of mechanic and numeric analyses. In order to determine the transition point, the preliminary tests on dilatometer according to real welding cycle were carried out. In connection to that, the heat affected zone on specimens, 48 pieces with the dimensions of 11x11x80 mm and 6 pieces with the dimensions of Ø12x100 mm, with the Gleeble 3500 were mechanically simulated. Two different welding cycles were applied, with the same peak temperature: $T_{p1}=1300^{\circ}\text{C}$, $T_{p2}=1100^{\circ}\text{C}$, but with different cooling time and interpass temperature; welding cycle 1: $t_{8/5}=20\text{s}$, $T_0=260^{\circ}\text{C}$; welding cycle 2: $t_{8/5}=12\text{s}$, $T_0=150^{\circ}\text{C}$. The specimens were afterwards heat treated at 730°C , once for 8 hours and once for 24 hours. Thereafter, the specimens for impact tests and tensile test specimens respectively were processed. The selected samples were investigated under the light microscope for microstructure characterisation and in the scanning electron microscope for fracture surface characterisation. From the light microscope images, the grain size measurements were carried out in the simulated HAZ. Finally, another macro hardness test was carried out. The numerical analyses were carried out by means of the program MatCalc developed by Univ. Prof. Dr. Ernst Kozeschnik. The equilibrium simulation and simulation of precipitation kinetics were performed.

1. INTRODUCTION

In order to keep the CO_2 emissions as low as possible and to reduce environmental pollution, a modern thermal power plant has to work with higher efficiencies. One way to meet these requirements is to use higher steam pressures and higher operating temperatures, which other ways leads to a greater mechanical and thermal stress on the material. Therefore, the used materials have to withstand higher pressures and temperatures, but at the same time they need to be economical and better weldable.

One of the solutions to solve this problem in some parts is the 9% chromium steel CB2 (*Figure 1*), a further development of P91 [1]. An important point for the improvement of the weldability of this material is the investigation and characterization of the heat affected zone (HAZ) [2, 3, 4]. To have a better overview, it is sometimes useful to simulate (Gleeble thermal simulation) a part of the HAZ, instead to investigate the HAZ of a real weld. The reason is quiet simple – a HAZ of a real weld is very narrow and mechanical tests are difficult to perform. On the other side, the width of a simulated HAZ can be user-defined and such HAZ is much easier to study.

At least, to complete the “picture” of the HAZ it is advantageous to investigate the precipitation kinetics in the HAZ beside the mechanical and metallurgical tests. A numerical simulation with the thermo-kinetic software MatCalc [5] is a good option for this kind of simulation.

Chem. element	[wt%]	Chem. element	[wt%]
C	0,14	Cu	0,06
Si	0,26	V	0,20
Mn	0,86	Nb	0,059
P	0,011	Ti	0,002
S	0,001	Al	0,018
Cr	9,52	Co	0,97
Ni	0,16	B	0,011
Mo	1,49	N	0,028

Figure 1. Chemical Analysis CB2 (voestalpine Gießerei Traisen GmbH)

2. EXPERIMENTAL PROCEDURE

2.1 Dilatometer test and Gleeble simulation

For the investigations of the HAZ with the *Gleeble 3500 simulator*, two different welding cycles and three post weld heat treatments (PWHT) were applied (*Figure 2*).

The welding (temperature) cycles (TC) have the same peak temperatures of 1300°C and 1100°C, but different cooling times (20 seconds for TC1, 12 seconds for TC2) and interpass temperatures (260°C for TC1 and 150°C for TC2).

To optimise the temperature cycles for the *Gleeble 3500 simulator*, *dilatometer tests* were made. The aim of these tests was to see the transformation behaviour of the material and to use this data for *Gleeble 3500*, but also for *MatCalc* numerical simulations.

The results of the dilatometer tests were evaluated with the Tangent-Method [6, 7]. Mean values were calculated (*Figure 3*) and used to determinate the peak and interpass temperatures.

Series	Temp. cycle	PWHT
S19	TC1	as simulated
S20	TC2	as simulated
S21	TC1	730°C/8 hours
S22	TC1	730°C/24 hours
S23	TC2	730°C/8 hours
S24	TC2	730°C/24 hours

Figure 2. Investigation matrix

	Temp. cycle 1	Temp. cycle 2	Mean values
A_{c1} [°C]	965	925	945
A_{c3} [°C]	1100	975	1035
M_s [°C]	365	365	365
M_f [°C]	155	185	170

Figure 3. Dilatometer test - mean values

Afterwards, the *Gleeble*-simulated samples were mechanical and metallurgical studied according to corresponding standards.

2.2 Mechanical tests

The *tensile tests* were made according DIN 50125, the specimens had the Form B. It was important that the specimens break in the *Gleeble*-simulated area (simulated HAZ). For this reason, the diameter (d_0) was reduced from 8 mm to 7 mm in this area (*Figure 4*).

As shown in *Figure 5*, the material tensile strength is not depending on the temperature (welding) cycle but on the PWHT duration. The highest strength is reached in “as simulated” condition (without PWHT), around 930 N/mm². The tensile strength is decreasing with a longer

PWHT duration, as expected. For the 8 hour heat treatment, tensile strength has the same value for both temperature cycles – 789 N/mm². A longer heat treatment (24 hours) has a lower tensile strength as result – around 735 N/mm².

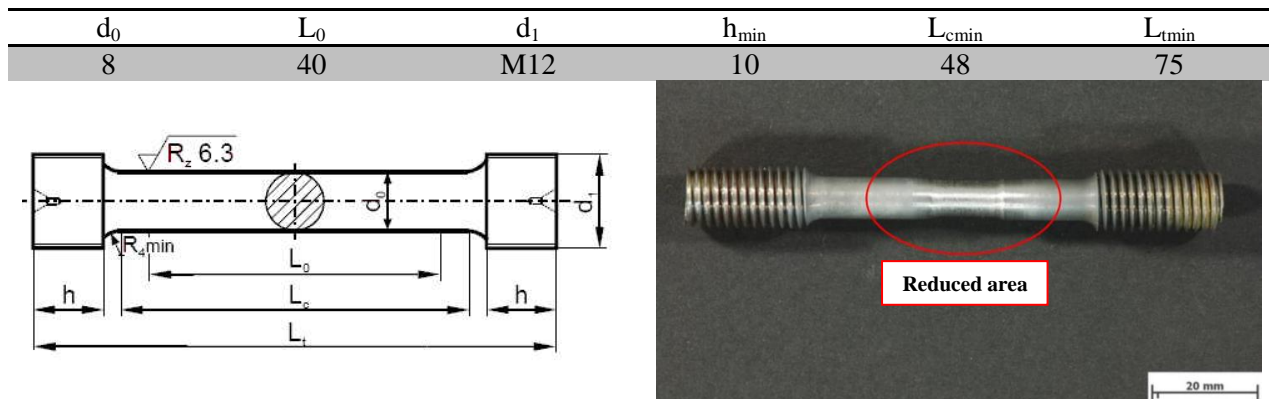


Figure 4. DIN 50125 Form B tensile specimens and the specimen with reduced area

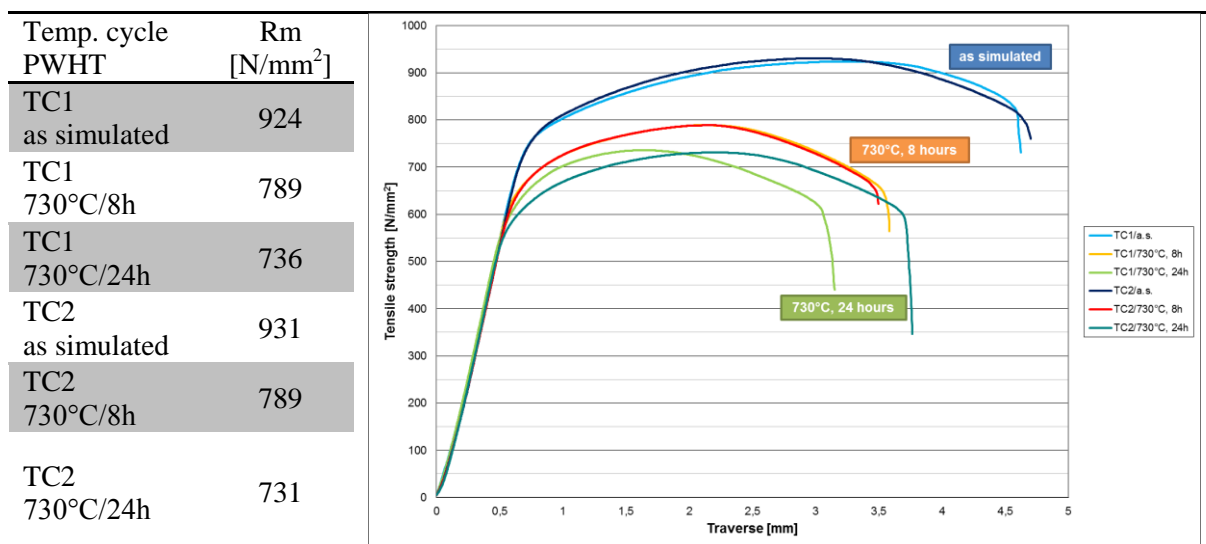


Figure 5. Tensile tests

The toughness of the material was investigated in the *instrumented impact test* according to EN ISO 14556. The instrumented impact test is carried out in the same way as the Charpy impact test according to EN ISO 148-1, but a force-deflection curve (*Figure 6*) is also determined during this experiment. The surface under this curve corresponds to the impact energy of the sample:

$$A_v = \int_{s_2}^{s_1} F(s) ds \text{ [J]}$$

The test procedure is performed with a pendulum impact tester whose hammer pen is equipped with instrumentation for the determination of force-time curves. The deflection-time curve is determined either by a rotary encoder or a measuring device for determination of the way below the sample. According the standard, there are 6 different types of force-deflection curves (A to F). The Type A is typical for a very brittle specimen, the Type F a very ductile. The curves are recorded and evaluated by the software „Perception“.

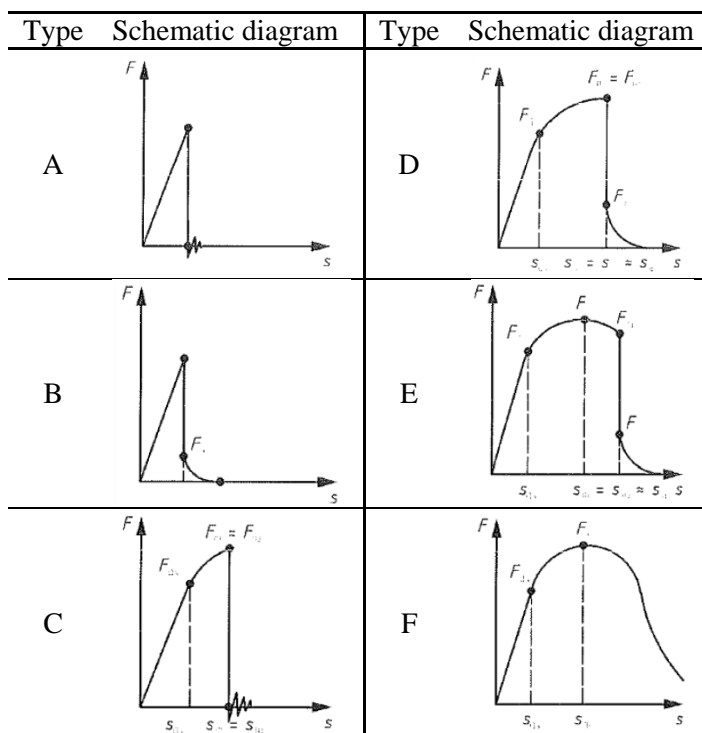


Figure 6. Typical force-deflection curves EN ISO 14556

for TC1 and 13 Joules for TC2 at -10°C , in the upper shelf 84 Joules respectively 76 Joules at 200°C .

The highest impact strengths were reached with the longer heat treatment ($730^{\circ}\text{C}/24$ hours). The transition zone was nearly the same as for the shorter heat treatment (ca. 60°C). In the lower shelf, the impact values were between 8 Joules and 16 Joules for TC1 and 9 Joules for TC2 at -30°C , in the upper shelf 80 Joules respectively 101 Joules at 200°C .

To estimate the width of the simulated HAZ, *Vickers hardness tests* were carried out. Two different hardness tests were performed (Figure 7):

- Line measurement with HV1 and HV10 to estimate the width of the simulated HAZ, and afterwards
- 3-point measurement with HV10 to estimate the hardness of the simulated HAZ.

The line measurements with HV1 and HV10 are corresponding very well. The highest hardness is around 280 HV1 (Figure 7 left). Due to the hardness drop at around 12 mm, we can differentiate the simulated HAZ and the base material. It can be seen, that the simulated HAZ is followed by a softening zone, which has a lower hardness for around 20 HV1 than the base material.

After determination of the simulated HAZ width, 3-point measurements were made. Because the line measurement was made on a specimen simulated with TC2 and $730^{\circ}\text{C}/8\text{h}$, a 3-point measurement of this specimen was not performed. As we can see in Figure 8, the as simulated specimens had an obvious higher hardness (ca. 460 HV10) compared to the heat treated specimens (283 HV10, respectively 261 HV10). The temperature (welding) cycle has less effect on the hardness.

Hofer-Hung curves for the impact tests were also made. The highest impact values were reached with the second temperature cycle (TC2 – faster cooling time, lower interpass temperature) combined with the PWHT of $730^{\circ}\text{C}/24$ hours – 101 Joule at 200°C , the lowest also with TC2 but in “as simulated” condition – 3 Joule at -30°C .

The transition zone for the “as simulated” specimens was around 100°C for the first temperature cycle (42 Joules). The impact values in the lower shelf were 4 Joules at -30°C and 5 Joules at room temperature, in the upper shelf 81 Joules at 200°C . For the second temperature cycle, upper shelf was not reached even at 200°C – 49 Joules.

The specimen heat treated at 730°C for 8 hours had a transition zone at around 60°C for both temperature cycles. The impact values in the lower shelf were 8

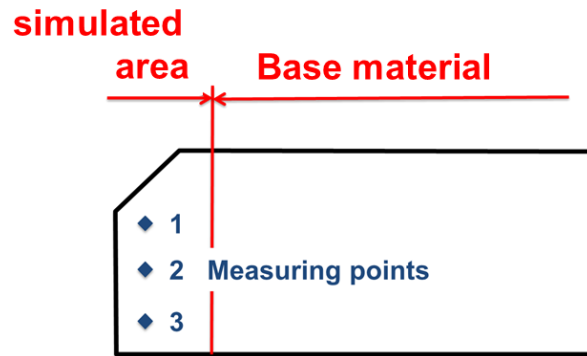
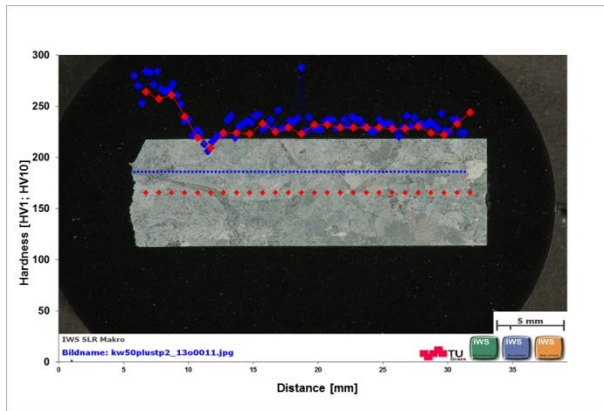


Figure 7. Hardness tests (left: line measurement; right: 3-point measurement)

Measuring point	TC1	TC2	TC1	TC1	TC2
	as simulated	as simulated	730°C/8h	730°C/24h	730°C/24h
1	476	465	276	268	263
2	452	452	282	257	254
3	449	454	290	259	266
Mean value	459	457	283	261	261
Standard deviation	12,1	5,7	5,7	4,8	5,1

Figure 8. 3-Point-measurement (HV10)

2.3 Metallurgical tests

After the impact test, representative specimens from each series (temperature cycle and PWHT) were chosen for metallurgical investigations. One half of the impact test specimen was used for microstructure characterisation (light microscope) and the other half for fracture surface characterisation (scanning electron microscope).

For the light microscopy, samples were prepared as usual for these tests. They were grinded down with different abrasive papers (FEPA Norm grain size from 240 till 4000) and afterwards polished with diamond paste (grain size 3 μm and 1 μm). After polishing, the specimens were ultrasonic cleaned for 15 minutes. To obtain a blank and clean surface, suitable for metallurgical investigations, the specimens were at last polished for a second time in a vibration polishing machine for 12 hours. Without this second polishing loop, it was not possible to see the microstructure with used etchant – modified Lichtenegger-Bloech III etchant. To prepare this etchant, 100 ml distilled water has to be warmed up to 50°C. To the warm distilled water 0,75 g ammonium bifluoride and 0,90 g potassium metabisulfite has to be added. Constant stirring of the etchant is necessary. The specimen was inserted into the etching bath and easily moved during etching. The etching time depends on the etching temperature and varies from 7 seconds in a very fresh etching solution to 20 seconds when the solution was not fresh any more. Accordingly, a time tracking was pointless. The sample should be etched as long as the sample surface becomes a slight brown colour. According the literature wet etching is recommended, but a subsequent drying of the specimens proved to be purposeful.

As seen in Figure 9, the simulated specimens have a typical martensitic structure. The grain borders are easy to identify for the heat treated specimens, but not for the as simulated. Therefore, it was not possible to determine the grain size of the as simulated specimens. The main values of the grain size for the heat treated specimens were 19 μm (730°C/8h) and 9 μm (730°C/24h) for the first temperature cycle, respectively 11 μm and 7 μm for the second. On the grain boundaries are carbides and we can see pores and inclusions from the casting process. These were easier to see in non-etched state, the cracks in the simulated area are clearly visible in etched state (Figure 10). With the additional heat treatment microstructure loses its recognisable cast structure, it becomes much finer.

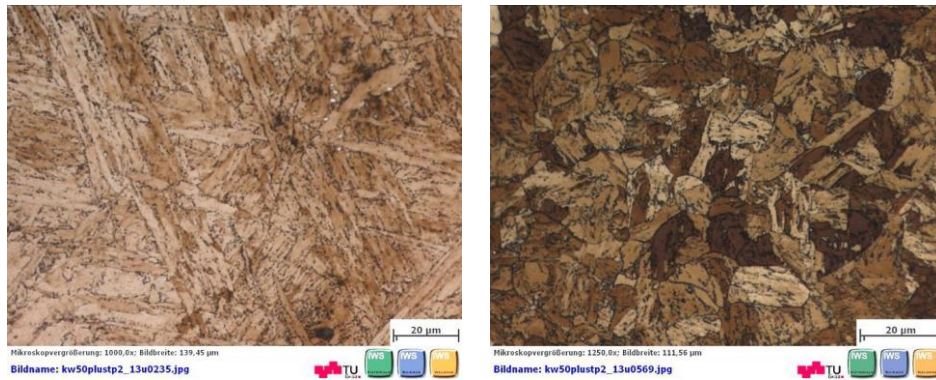


Figure 9. CB2 simulated area microstructure (left: as simulated; right: 730°C/24 hours)

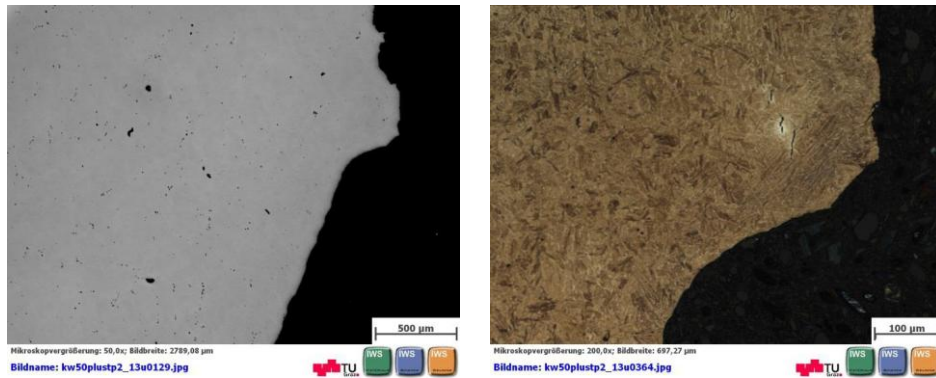


Figure 10. Pores, inclusions and cracks in the simulated area (as simulated specimen)

In the *scanning electron microscope*, specimens with very low and those with higher impact values were compared to each other. The fracture surface of brittle specimens under the microscope (Figure 11 right) was flat with just a few ductile areas. In the macro picture (Figure 11 left) a strong reflective fracture surface was observed. On the other side, the specimens with higher toughness had a dull fracture surface (Figure 12 left), which is a sign of plastic deformation behaviour before breaking. Honeycomb structure is a typical sign for the ductile areas and at the bottom of this structure particles were identified (Figure 12 right). Mayr [8] identified these particles as boron nitrides.

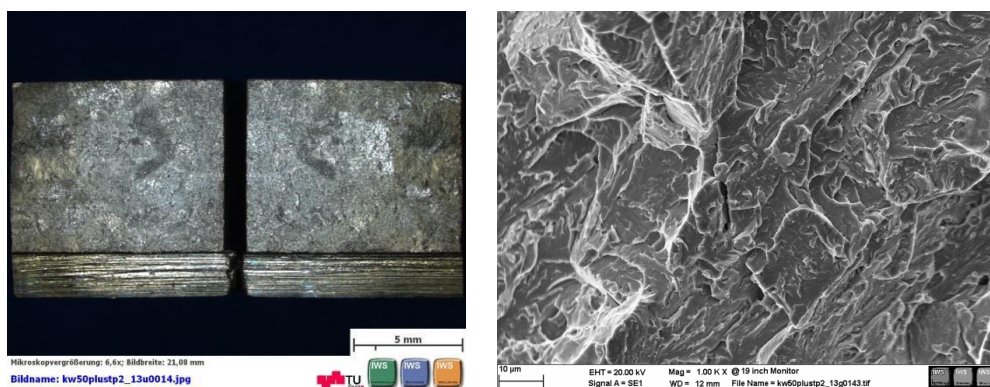


Figure 11. Macro and SEM – TC1, as simulated

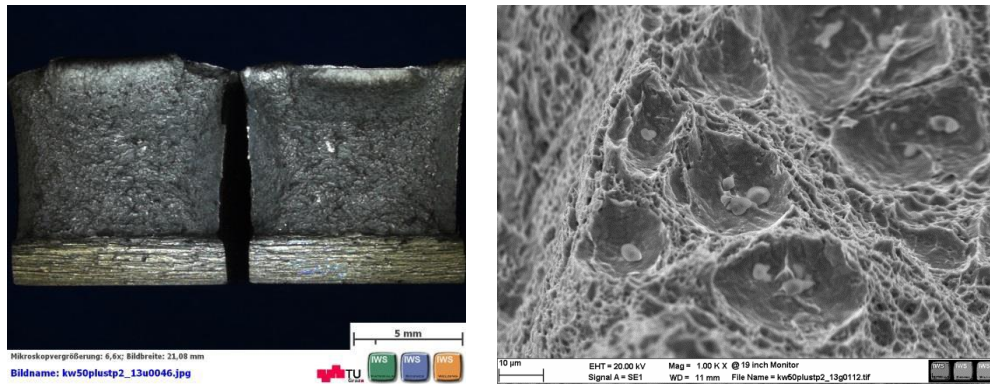


Figure 12. Macro and SEM – TC2, 730°C/24h

2.4 Numerical simulation

Heat treatments, welding cycles and service (operating) conditions have a influence on the microstructure. With the software MatCalc (MATERial CALCulator) it is possible to make a thermodynamically equilibrium simulation, Scheil calculation (solidification simulation), a simulation of the precipitation growth according thermodynamically laws etc. The theoretical background of the software is the calculation of the Gibbs energy of the system [9]. Phase fraction, mean radius and number density of precipitates were calculated as a function of time.

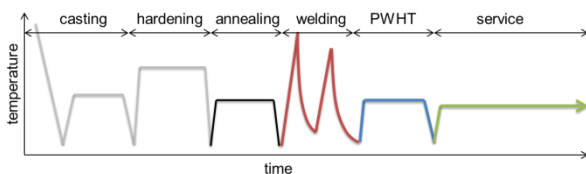


Figure 13. Temperature control MatCalc

used for the welding simulation. Post weld heat treatment was in each case adapted to the real conditions (730°C for 8 hours and for 24 hours) and the service time was simulated for 100 000 hours at 625°C.

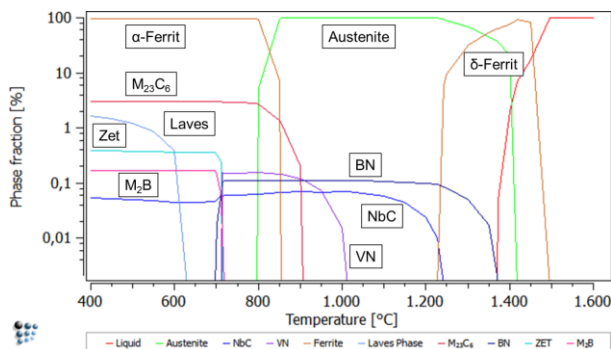


Figure 14. Equilibrium calculation MatCalc

precipitations occur as vanadium nitride (VN) and niobium carbide (NbC). NbC occur at approximately 1250°C to room temperature, VN at 1000°C and it is replaced by the Z phase at 710°C.

The development of precipitates over time was simulated in a total of five temperature cycles, as shown in Figure 13. The precipitates condition for booth temperature cycles after PWHT is shown in Figure 15. Compared are the phase fractions and the mean radius of the relevant precipitation phases.

Figure 13 shows the temperature control of the production of a cast component. The same temperature control was used for the heat management of the numerical simulation. For the casting, hardening and annealing simulation, temperature cycles from the real production process were used. Temperature cycles from the thermomechanical simulation (Gleeble) were

According the equilibrium simulation, Figure 14, austenite transformation starts at 796°C (A_{e1}) and ends at 856°C (A_{e3}). The ferrite occurs till A_{e3} as α -ferrite; upon cooling it occurs as δ -ferrite (till 1230°C). Main precipitation phases are $M_{23}C_6$ (from room temperature to around 900°C), the intermetallic laves phase (from room temperature to around 630°C) and the Z phase (between room temperature and around 710°C). Boron nitride (BN) is between 400°C and 1350°C stable, from 700°C to room temperature M_2B is more stable the BN. The MX precipitations occur as vanadium nitride (VN) and niobium carbide (NbC). NbC occur at approximately 1250°C to room temperature, VN at 1000°C and it is replaced by the Z phase at 710°C.

PWHT	Phase fraction [%]				Mean radius [nm]			
	TC1	TC1	TC2	TC2	TC1	TC1	TC2	TC2
	8 h	24h	8 h	24h	8 h	24h	8 h	24h
Laves	0	0	0	0	1	1	1	1
M ₇ C ₃	0	0	0	0	0	1	1	1
M ₂₃ C ₆	3,06	2,89	3,11	3,03	195	194	161	199
BN	0,11	0,11	0,11	0,11	141	1514	82	1332
VN	0,06	0,13	0	0,07	16	25	0	28
NbC	0,06	0,07	0,05	0,07	91	94	141	153

Figure 15. Phase fraction and mean values of the precipitates after PWHT

Changes of welding parameters show any strong effects on the phase fractions of the precipitates after PWHT according simulation. On the other hand, the simulation shows, that a longer PWHT substantial increase of BN and a slight coarsening of the M₂₃C₆ mean radius. On the MX mean radius, the PWHT time has just a small influence. In view of the temperature (welding) cycles with different cooling rates ($t_{8/5}$ time) and interpass temperature, slight differences in the mean radius of M₂₃C₆ and BN are determined. The MX precipitates, especially VN, does not create with a higher cooling time and shorter PWHT. The M₇C₃ precipitates dissolve during PWHT in favour of M₂₃C₆ precipitates.

The grain size has an effect on the simulation results. In the simulations carried out, the grain size was assumed to be constant. In reality, the grain size is ca. 1500 μm in the base material and ca. 20 μm in the HAZ. At this time, the numerical models in the background do not provide an opportunity to consider this development in MatCalc simulation.

3. CONCLUSION AND OUTLOOK

The studied activities have shown that the results remain highly dependent on the post weld heat treatment and less from the welding cycle. This became clear in the tensile tests and hardness measurements, where in “as simulated” specimens higher values were measured.

This statement is not directly applicable to the instrumented Charpy impact tests. The highest values were obtained with the long heat treatment (730°C/24 hours). However, the instrumented impact tests must be evaluated differently, since the curve progression plays a greater role for the characterisation of the fracture behaviour as the integral over the curve. Post weld heat treatment has a higher influence on the toughness as the used welding cycle – higher impact values were achieved with longer heat treatments.

The heat treatment also affects the microstructure. The grain size measurement has shown that a longer heat treatment refines the microstructure. According the results, welding cycles have an influence on the grain size too. The grain size of the second welding cycle (TC2) was finer in both heat treatment variants than with the first welding cycle (TC1). However, these results should be confirmed with alternative measurement methods.

The numerical simulations showed small differences between the welding cycles among themselves, at least in the phase fractions. Differences are encountered in the mean radius and particle densities. After a long service time simulation, no differences depending on the welding cycle or heat treatment were observed.

The first step in future studies of the HAZ should be a more accurate picture of temperature cycles used for dilatometer tests and Gleeble simulation, especially with regard to the heating rates. The transformation temperatures should be more precisely determined in dilatometer on basis of several measurements. This is especially for the MatCalc numerical simulation very important.

Regarding the instrumented impact tests, as indicated, there is a lot of potential for improvement. The used software “Perception” had bugs during the tests and needs to be updated by

the manufacturer. The software calculated impact values had in some cases unacceptable deviations to the analogue measured values (acceptable deviations according standard are ± 5 Joule) [10].

Since it was impossible to determine the grain size of the “as simulated” specimens, suitable etchants should be found, or developed, which may make the grain boundaries more visible. Alternatively evaluations with the ASTM network should be carried out to compare the results of these tests and the tests evaluated with the used software KS400.

The simulation of grain size changes and dislocation density changes in MatCalc, simultaneously with the simulation of precipitation kinetics, was in the used MatCalc version (5.60.0005) not possible. They were therefore assumed to be constant during the simulations. This point should be an important research subject for the MatCalc developers.

The multilayer welding was simulated with a double cycle. A triple cycle, or even quadruple cycle, would provide a more accurate picture of the HAZ.

EDX and TEM studies for the verification of the MatCalc simulation results could be a next step.

4. BIBLIOGRAPHY

- [1] M. Staubli, COST 522 Steam power plant Final Report 1998-2003, 2003.
- [2] A. Sarić, Charakterisierung von Merhlagenschweißungen, Institut für Werkstoffkunde und Schweißtechnik, TU Graz, 2014.
- [3] S. Baumgartner, M. Schuler, C. Ramskogler, E. Schmidtne-Kelity, A. Sarić, R. Schnitzer, C. Lochbichler and N. Enzinger, Mikrostrukturentwicklung von CB2 Fülldraht-Schweißungen, VDEh, 2013.
- [4] S. Baumgartner, A. Holy, M. Schuler, A. Sarić, R. Schnitzer and N. Enzinger, Properties of a creep resistant 9Cr-1.5Mo-1Co cast steel joint welded with a matching flux-cored wire, *Welding in the World*, 2014.
- [5] E. Kozeschnik, “MatCalc,” TU Wien, [Online]. Available: <http://matcalc.tuwien.ac.at>, Zugriff: 18.02.2014 [Accessed 08 02 2014].
- [6] H. B. H. Yang, Uncertainties in dilatometric determination of martensite start temperature, *Materials Science and Technology*, 2007.
- [7] A. Farahat, Dilatometry determination of phase transformation temperatures during heating of Nb bearing low carbon steels, *Journal of Materials Processing Technology* 204, 2008.
- [8] P. Mayr, Evolution of Microstructure and Mechanical Properties of the Heat Affected Zone in B-Coontaining 9% Chromium Steels, Graz: Institut für Werkstoffkunde und Schweißtechnik, Technische Universität Graz, 2007.
- [9] E. Kozeschnik, Thermodynamische Berechnung der Phasengleichgewichte und der Ausscheidungskinetik in Metallischen Werkstoffen, Graz: Institut für Werkstoffkunde und Schweißtechnik, Technische Universität Graz, 1997.
- [10] EN ISO 14556: Stahl - Kerbschlagbiegeversuch nach Charpy (V-Kerb) - Instrumentiertes Verfahren, 2007.